

An-Najah National University

Faculty of Graduate Studies

**Sensitization of semiconducting nano powder catalysts
in photodegradation of medical drugs and
microorganisms in water**

by

Fedaa Talal Saleh

Supervisor

Prof. Hikmat Hilal

**This Thesis is Submitted in Partial Fulfillment of the Requirements for
the Degree of Master of Science in Chemistry, Faculty of Graduate
Studies, An- Najah National University, Nablus, Palestine.**

2011

**Sensitization of semiconducting nano powder catalysts
in photodegradation of medical drugs and
microorganisms in water**

by

Fedaa Talal Saleh

This Thesis was defended successfully on 24 /11 / 2011 and approved by:

Committee Members

Signatures

- | | | |
|----------------------------------|----------------------------|-------|
| 1- Prof. Hikmat S. Hilal, | (Supervisor) | |
| 2- Dr. Hatim salim | (External Examiner) | |
| 3- Dr. Ahed Husni Zyoud | (Internal Examiner) | |

DEDICATION

I dedicate this thesis to:

* To my parents,

* My Husband Aysar Faydi

* My brothers and sisters

And

* To all my friends...

ACKNOWLEDGMENT

First I wish to thank my supervisor Prof. Hikmat Hilal for help, encouragement and guidance throughout my research work. I would also thank many people who gave me help and logistic support including Dr. Ahd Zyoud (for special help with polarography), Dr. Majdi Dwekat (for help with microbiology), Dr. daeHoon Park, Dansuk, South Korea and Jung-Euan KIM of ISSA, Chungju, south Korea (for measuring SEM and XRD), and Dr. Guy Campet of ICMCB, Bordeaux (for SEM and XRD measurements). I wish also to thank our lab technician Mr. Nafez Dweikat, for continued help and support.

The author wishes to express special thanks for friends Hiba Nassar and Manar Atallah for standing besides me throughout different stages. Thanks are also due to my parents and my husband for continued encouragement.

الإقرار

أنا الموقع أدناه مقدم الرسالة التي تحمل العنوان :

Sensitization of semiconducting nano powder catalysts in photodegradation of medical drugs and microorganisms in water

أقر بأن ما اشتملت عليه هذه الرسالة إنما هي نتاج جهدي الخاص، باستثناء ما تمت الإشارة إليه
حيثما ورد، وأن هذه الرسالة ككل، أو أي جزء منها لم يقدم لنيل أية درجة أو لقب علمي أو بحثي
لدى أية مؤسسة تعليمية أو بحثية أخرى .

Declaration

The work provided in this thesis , unless otherwise referenced , is the
researcher's own work , and has not been submitted elsewhere for any other
degree or qualification.

Student's Name :

اسم الطالب :

Signature :

التوقيع:

Date:

التاريخ:

List of Contents

Chapter one	Introduction	Page
	DEDICATION	III
	ACKNOWLEDGMENT	IV
	Declaratio	V
	List of Tables	VIII
	List of Figures	IX
	Abstract	XI
1.1	Overview	1
1.2	Semiconductor photo catalyst	2
1.3	Titanium dioxide TiO ₂	3
1.3.1	TiO ₂ photo catalytic activity process	5
1.3.2	Sensitization of TiO ₂	8
1.4	Anthocyanin	11
1.5	Phenazopyridine	13
1.6	E-colie bacteria	13
1.7	Staphylococcus aureuse	14
1.8	Objectives	15
Chapter two	Experimental	
2.1	Materials and chemicals	16
2.2	Instruments	16
2.2.1	UV/vis spectrophotometer	16
2.2.2	Polarograph	16
2.2.3	Fluorescence spectrophotometer	17
2.2.4	Lux-meter	17
2.2.5	XRD	17
2.2.6	SEM	17
2.3	Catalyst preparation	18
2.3.1	Preparation of TiO ₂ powder	18
2.3.2	Extraction of anthocyanin dye	18
2.3.3	Preparation of anthocyanin/ TiO ₂	18
2.3.4	Preparation of AC/ TiO ₂ /anthocyanin	19
2.3.5	Stock solution preparation	19
2.4	Calibration curve	20
2.5.1	Photo catalytic experiment	20
2.5.2	Control experiment	21
2.6	Photo catalytic degradation of phenazopyridine	21
2.6.1	Effect of pH	22
2.6.2	Effect of contaminant concentration	22
2.6.3	Effect of temperature	22
2.6.4	Effect of catalyst concentration	22
2.7	Photo catalytic degradation of bacteria	23
2.7.1	Material and equipment	23

VII

2.7.2	Photo catalytic experiment	23
Chapter three	Results and Discussion	25
3.1	Characterization results	25
3.1.1	XRD	25
3.1.2	SEM	26
3.1.3	Photoluminescence	28
3.1.4	UV-visible characterization	29
3.1.5.	anthocyanin characterization	31
3.2	Photo catalytic degradation of phenazopyridine	32
3.2.1	Calibration curve	33
3.2.2	Control experiment results	33
3.2.3	Photo catalytic experiment results	34
3.2.3.1	Effect of pH	35
3.2.3.2	Effect of contaminant concentration	39
3.2.3.3	Effect of temperature	41
3.2.3.4	Effect of catalyst concentration	45
3.3	Photodegradation of Bacteria	47
3.4	Conclusions	50
3.5	Suggestions	51
	References	52
	المخلص	ب

VIII

List of Tables

Table	Title	Page
1.1	Forbidden energy band gap values for common semiconductors	3
3.1	XRD data for prepared TiO ₂ compared with anatase and rutile	26
3.2	Values of %degradation, turnover number (TN), turnover frequency (TF) and quantum yield (QY) measured for phenazopyridin degradation after 100 min	38
3.3	Values of TN, TF, QY, and %phenazopyridine degradation for catalytic runs using different contaminant concentration.	40
3.4	Values of TN, TF, QY and %phenazopyridine degradation for catalytic runs using different temperatures	42
3.5	Values of ln (rate) vs. 1/T for phenazopyridine photodegradation experiments.	45
3.6	Values of, TN, TF, QY and %phenazopyridine degradation for catalytic runs with different catalyst concentration.	47
3.7	E-coli bacteria counting under different experimental conditions	47
3.8	Staphylococcus aureus bacteria counting under different experimental conditions	48

List of Figures

Figure	Title	Page
1.1	Schematics showing different crystal structures for TiO ₂	4
1.2	Schematics showing energy band gaps and redox potentials for common semiconductors	5
1.3	Schematics showing electron-hole pair formation in a semiconductor particle, a) before excitation, b) after excitation	6
1.4	Proposed mechanism for catalytic photoreactions onto TiO ₂ surfaces.	7
1.5	A schematic showing effect of doping with nitrogen on band structures for TiO ₂	9
1.6	A schematic showing sensitization of TiO ₂ in photo-degradation processes.	9
1.7	Structural formula for anthocyanin structure, a) in the free form, and b) anchored to TiO ₂ surface.	12
1.8	Structural formula for phenazopyridine	13
1.9	E-Colie bacteria	14
1.10	Gram stain of <i>S. aureus</i> cells	15
3.1	X-ray diffraction pattern for A: TiO ₂ , B : TiO ₂ /anthocyanin, C: TiO ₂ /anthocyanin/AC	25
3.2	SEM images for A) TiO ₂ , B) TiO ₂ /anthocyanin, C) TiO ₂ /anthocyanin/AC	28
3.3	Photoluminescence spectra measured for TiO ₂ : a) prepared, and b) commercial samples	29
3.4	Solid state electronic absorption spectra measured for (a):TiO ₂ ,(b): TiO ₂ /anthocyanin	30
3.5	Solid state electronic absorption spectra measured for anthocyanin dye.	31
3.6	TLC shows one components from extracted dyes.	32
3.7	Polarography calibration curve showing current vs. contaminant concentration	33
3.8	The main four equilibrium forms of anthocyanin existing in aqueous media.	36
3.9	Effect of pH on phenazopyridine photodegradation rate. All measurements were made at room temperature in aqueous solutions (50 mL) using 40 ppm starting contaminant solution, and AC/TiO ₂ / anthocyanin (0.10 g).	37
3.10	Effect of contaminant concentration on %photo-degradation at room temperature and pH 3.5.	40
3.11	Effect of temperature on phenazopyridine photo-degradation rate	42
3.12	Reaction profiles showing contaminant concentration with time at different temperatures.	43
3.13	Plots of ln (rate) versus 1/T for photo-degradation of	45

	phenazopyridine.	
3:14	Effect of catalyst concentration at room temperature, pH 3.5	46
3:15	Percent of photodegradation of E-coli bacteria using TiO ₂ and TiO ₂ / anthocyanin	48
3:16	Percent of photodegradation of <i>Staphylococcus aureus</i> bacteria using TiO ₂ and TiO ₂ / anthocyanin.	49

**Sensitization of semiconducting nano powder catalysts in
photodegradation of medical drugs and microorganisms in water**

By

Fedaa Talal Saleh

Supervisor

Prof. Hikmat Hilal

Abstract

Photocatalytic degradation of organic contaminants in water and air has great deal of attention. TiO_2 is the most widely used semiconductor photocatalyst due to its high photo-stability, non-toxic nature, high oxidizing potential and its water insolubility under different conditions. In this research TiO_2 nano-particles were prepared from TiCl_3 . Then they were sensitized by anthocyanin natural dye extracted from Hibiscus (Karkade). The TiO_2 /dye system was used as photocatalyst to degrade water contaminant such as phenazopyridine and E-coli bacteria under spot halogen lamp irradiation. TiO_2 was characterized by measuring the XRD, SEM, Photoluminescence, UV-visible spectra. Effects of different parameters on catalyst efficiency were studied such as pH effect, contaminant concentration, catalyst concentration and temperature. The efficiency of catalyst increased with increasing the concentration of contaminants, the concentration of catalyst and pH value. In this research the photodegradation reaction was slightly temperature dependent. Details of phenazopyridine degradation study are presented here, together with a brief screening investigation of bacteria degradation.

Chapter One

Introduction

1.1 Overview:

Water is one of the prime elements responsible for life on earth, 70% of earth surface is covered by water, and 75% of the human body is water .

modern life, industrial development and agriculture cause decrease in water availability for human and increase water contamination. Drinking

water today is not pure and contains a lot of chemicals, bacteria, viruses, and inorganic minerals; this promoted scientists to develop different ways to purify water [1- 2]. Many water purification methods were followed in recent years, including physical, biological and chemical processes, are known. Physical processes were applied to remove the solids from liquids through different filtration techniques. Biological processes were applied to decompose dissolved organic compounds. That was achieved using microorganisms, such as bacteria that have ability to use these organic compounds to provide energy for microbial metabolism [3].

UV radiation was also used in disinfection. The short wave length radiations (UV) destroy the nucleic acids in the microorganisms and kill them [4].

Chemical processes involve adding chemicals for different purposes such as chelating agents, oxidizing agents, and reducing agents, in clarification and disinfection [5-6]. Advanced oxidation processes are newer chemical techniques used for water purification. Their work involves generation of highly reactive free radicals, such as hydroxyl radical which is effective in destroying organic chemicals. They have relatively high oxidation potential (2.33V) and their rate of oxidation reaction faster than convention oxidation processes. The most important advanced oxidation processes are:

1-H₂O₂/ UV processes, in this process UV light is used to cleave O-O bond in hydrogen peroxide then generate the hydroxyl radical [7-10].

2-Fentons reactions, where OH[·] comes from the reaction between ferrous iron and hydrogen peroxide [11- 12].

3-TiO₂\UV process, UV light here excites the TiO₂ to produce OH[·] in a mechanism described later [9].

1.2 Semiconductor photo-catalysis:

The process of heterogeneous photocatalysis involves semiconductors. It was developed during the last fourty years. Heterogeneous photo catalysis is defined by Palmisano and Sclafani (1997) as: “A catalytic process during which one or more reaction steps occur by means of electron –hole pairs photo generated on the surface of semiconducting materials illuminated by light of suitable energy” [13].

The initial interest in the heterogeneous photocatalysis started when Fujishima and Honda discovered in 1972 the photochemical splitting of water to hydrogen and oxygen on TiO_2 electrodes [14]. According to band theory each solid can be characterized by the energetic bands, valence band VB (highest occupied molecular orbital) and conduction band CB (lowest unoccupied molecular orbital). The distance between valence band and conduction band characteristic of the solid is called forbidden band (or energy band gap) E_g . In semiconductors the energy band gap ranges from 0.7-3.5 eV. Table (1.1) shows values of band gap of a number of known semiconductors [15]:

Table (1.1) Forbidden energy band gap values for common semiconductors [15].

Semiconductor	$E_g(\text{eV})$
Si	1.1
Fe_2O_3	2.3
CdS	2.5
WO_3	2.8
TiO_2 (rutile)	3.0
TiO_2 (anatase)	3.2
ZnO	3.2
SnO_2	3.5

1.3 Titanium dioxide TiO_2

Titanium oxide (TiO_2) is a transition metal oxide. It is widely used as a white pigment, in paints, plastics, paper and food industry [16]. TiO_2 is also used as catalyst for selective reduction of NO_x , effective decomposition of organic compounds and in many redox reactions. TiO_2 in nature is usually

associated with iron mostly as ilmenite. Ilmenite is used to produce TiO_2 by either of two processes: the sulphate process or the chlorine process [17-18]. The TiO_2 may exist in three different forms rutile, anatase and brookite. The structures of these three forms are shown in (Figure 1.1).

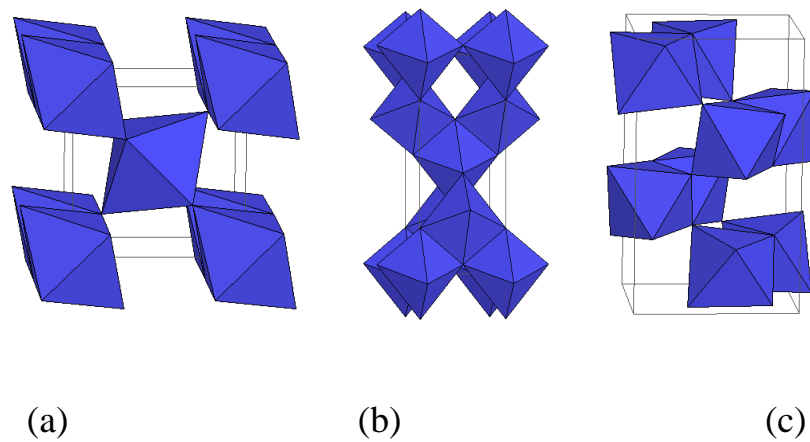


Figure 1.1: Schematics showing different crystal structures for TiO_2 (a) rutile (b) anatase (c) brookite[19].

TiO_2 is the most commonly semiconductor used in water purification due to its high photostability, non toxic nature, high oxidizing potential, insolubility in water under different condition and low cost. Rutile is the most stable form of TiO_2 , whereas anatase is the most catalytically active system [18, 20], due to it's more negative potential than rutile (Figure 1.2). This makes it more competitive than rutile for reduction reaction.

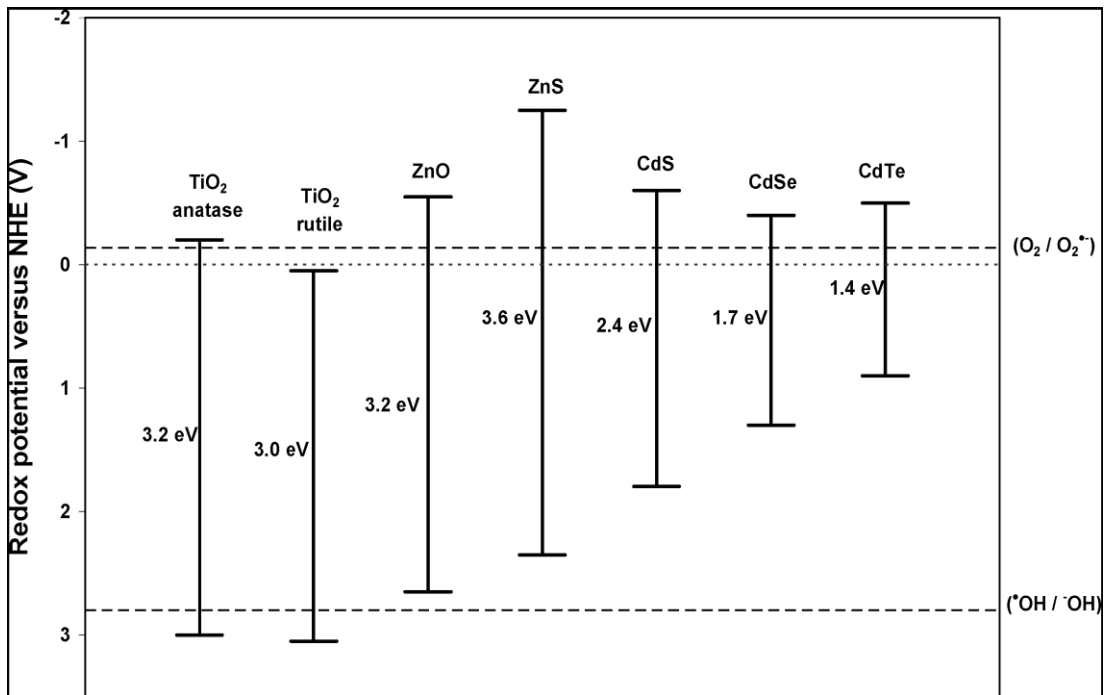


Figure 1.2: Schematics showing energy band gaps and redox potentials for common semiconductors [14].

1.3.1 TiO₂ photocatalytic activity process:

TiO₂ activated by UV light at wavelengths shorter than 387 nm can almost damage any organic compound. When TiO₂ particle absorbs a photon having energy greater than the band gap, the electron in the valence band will be excited to the conduction band. The result of such excitation will be electron-hole pair formation [14, 18]. (Figure 1.3) summarizes this model.

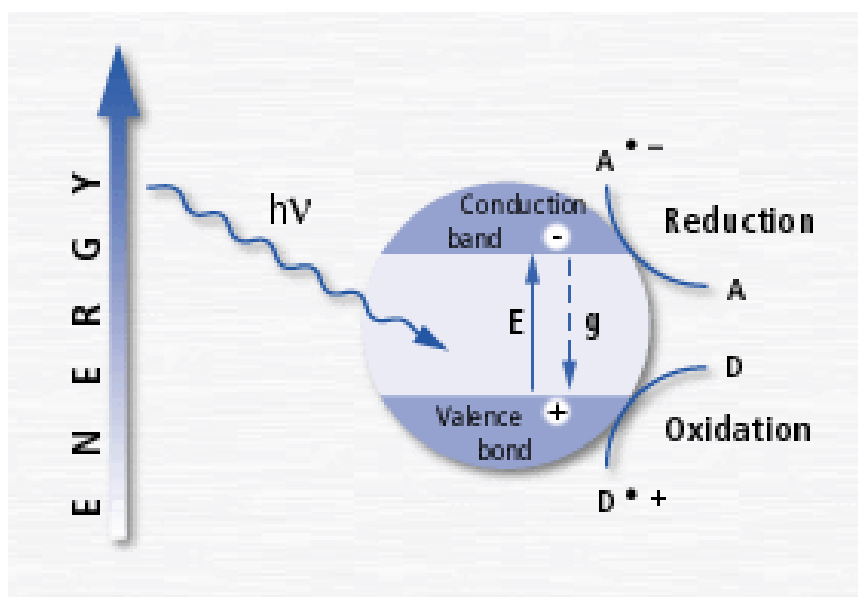


Figure 1.3: Schematics showing electron-hole pair formation in a semiconductor particle[21].

The hole, formed as a result of electron transfer from V.B. to C.B., has a potential to oxidize water and form a hydroxyl radical. The electron (in C.B.) rapidly reduces oxygen to form the superoxide anion. This can in turn react with water to form hydroxyl radical again. Hydroxyl radicals are very powerful oxidizers and can easily oxidize organic species ultimately to carbon dioxide and water. The process of photocatalysis reaction is explained in (Figure 1.4):

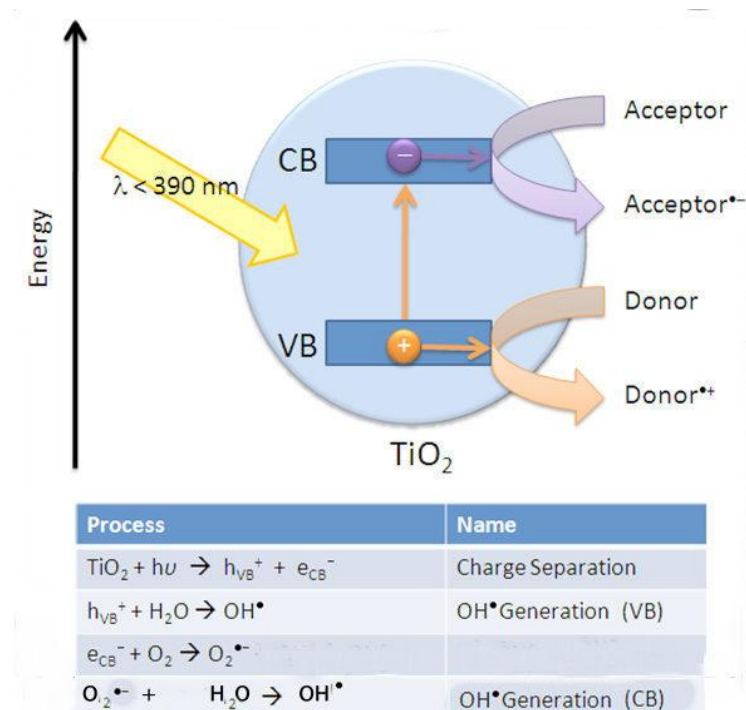
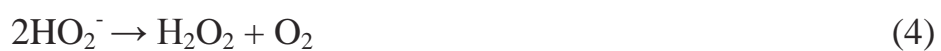


Figure 1.4: Proposed mechanism for catalytic photoreactions onto TiO₂ surfaces [22].

Based on (Figure 1.4), the oxidation of organic compounds may occur as shown in Equation (1.1) [23]:



The resulting radicals may undergo other nonproductive reactions as shown in equations (2-5)



For efficient photocatalysis to occur in a given catalytic mixture, the following features must be met:

- The surface bound water allows for efficient oxidation
- Water should be aerated to provide oxygen to the solution

The pollutant should be adsorbed or should be very close to the surface of the catalyst. When the surface area increase the number of adsorbed molecules should also increase. Nanoparticles have relatively high relative surface areas, compared to macro system. Therefore nanoparticles are very efficient in photocatalytic reaction [22]. TiO_2 nanoparticles were used in photodegradation by UV illuminating [24-25].

1.3.2 Sensitization of TiO_2 :

The limitation in using TiO_2 in degradation of organic compounds is that they absorb only in UV region. This means that we must use a supply for UV light; since only about 4% of the solar spectrum falls in UV region. To utilize solar energy the catalyst must be modified to absorb in the visible region. Different ways were followed to achieve this. One way involves doping TiO_2 with another element to reduce the band gap energy. For example nitrogen doped titanium dioxide has yellow color which means it will absorb visible light. The mechanism of enhancement by nitrogen doping is understandable, where nitrogen introduces a new occupied orbital

between C.B and V.B, (Figure 1.5). This new orbital acts as a step in electron jumping, so it reduces the energy band gap.

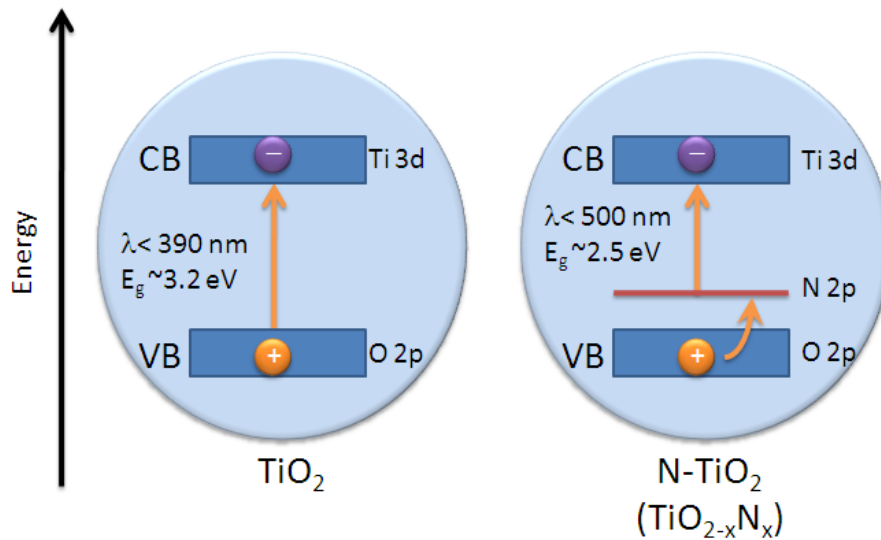


Figure 1.5: A schematic showing effect of doping with nitrogen on band structures for TiO_2 [22].

Another way used to reduce the energy is by sensitization with dye molecules. In this technique light absorption occurs by the dye molecule that is attached to the TiO_2 nano-particle, in visible region (Figure 1.6).

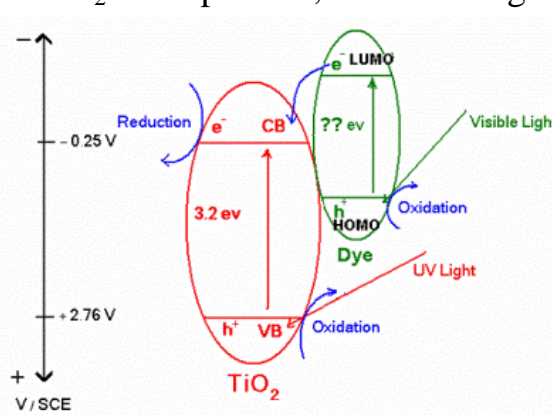


Figure 1.6: A schematic showing sensitization of TiO_2 in photo-degradation processes [26].

When the dye molecule absorbs a photon, its electron will be excited from HOMO level (Highest Occupied Molecular Orbital) to LUMO level (Lowest Unoccupied Molecular Orbital). This is followed by relaxation through electron loss to the TiO₂ conduction band [27]. The hole in the HOMO of dye will oxidize the organic species; spontaneously the electrons in the conduction band of the TiO₂ semiconductor will reduce other species (like O₂) or other contaminant cations. For electron relaxation to occur, the energy level of the LUMO must be higher than the conduction band edge of TiO₂, so that an electron can be injected during the relaxation process. The dye HOMO must also be lower (more positive) than the reduction potential of the organic contaminant.

Sensitization of semiconductors under solar light was firstly applied in solar cell and discovered by Oregan and Gratzel, both synthetic and natural dyes were used and give efficient results [28]. This sensitization was also applied in water purification. Synthetic dyes are widely used as sensitizers for semiconductors to degrade organic compounds, and so nano-crystal semiconductors that have a color like CdS.

CdS particles absorb in visible region, and gives efficient catalyst but gives hazardous effects on environment, since CdS decomposes to give Cd²⁺ toxic ions in solution.

Most of advanced oxidation processes need UV light. Some processes need to use metals, like Fenton's reaction that has bad effects to human body, in addition to its high cost [21].

In this work we prepare nano-particles of TiO_2 then sensitized them by natural dye (Anthocyanin). The anthocyanin was used because it is safe, available and not costly. The sensitizer dye must have hydroxyl groups to attach with TiO_2 surface in order to prevent its leaching into solution. Natural dyes as sensitizers have not been widely used in water purification field. In earlier work, screening study on degradation of some organic compounds using TiO_2 sensitized by anthocyanine dye was made [29]. This work involves such study in more detail. Effects of different parameters have now been studied. Reaction kinetics have been studied. Moreover, a screening study on bacteria photodegradation using this catalyst system has also been done here.

1.4 Anthocyanine:

Anthocyanin are water soluble pigments that occur in all tissues of higher plants including roots, stems, leaves, flowers and fruits. It's responsible for the red blue and purple color of many plants [30- 31]. It's one class of flavonoid compounds which are sugar bond polyphenols. They are odorless and nearly flavorless. Anthocyanin have important roles as antioxidants, since they captures the free radicals and neutralize them. There is also

considerable evidence that anthocyanin pigments and flavonoid have preventive and therapeutic roles in a number of human diseases [32] as:

- they have anti inflammatory properties which affect collagen and the nervous system
- There were many studies showing that mortality from heart diseases inversely correlated with flavonoids intake in diet.
- Anthocyanin have efficiency to inhibit some human tumor cells [31, 33-34]

Anthocyanins have another use. They are used in sensitized solar cell.

Anthocyanins have hydroxyl groups which anchor to the surface of TiO_2 in rapid reaction, displacing an OH^- counter ion from the Ti (IV), as shown in Figure (1.7).

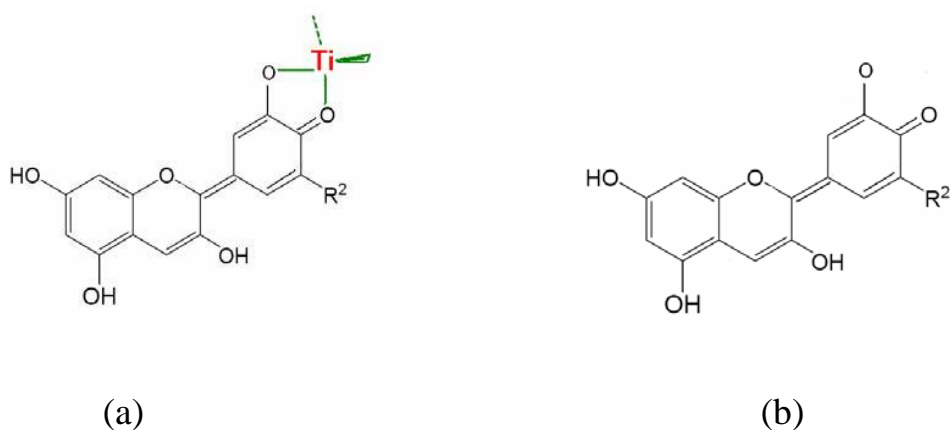


Figure 1.7: Structural formula for anthocyanin structure, a) anchored to TiO_2 surface and b) in the free form, [34].

Although anthocyanin captures the free radicals it still has different behaviors when attached to metals and exposed to light. Therefore, it may be help to produce free radicals under irradiation.

1.5 Phenazopyridine:

Phenazopyridine, is 2,6-diamino-3-(phenylazo)pyridine, (Figure 1.8). Solutions of phenazopyridine have yellow reddish color. It was discovered by Bernhard Joos. It is often used to alleviate the pain, irritation, discomfort, or urgency caused by urinary tract infections, surgery, or injury to the urinary tract [33, 35]. Phenazopyridine is being used in this work as a model contaminant to be photodegraded. This strategy is important for further practices aiming at purifying water from pharmaceutical wastes.

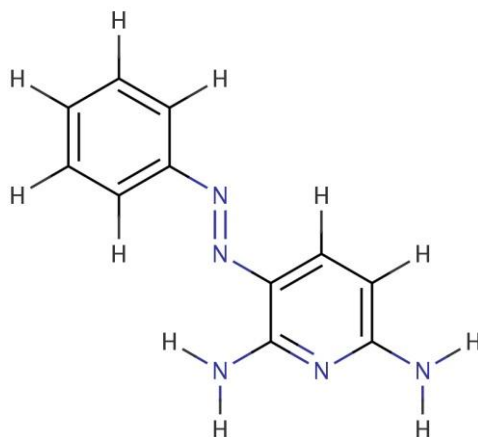


Figure 1.8: Structural formula for phenazopyridine[35].

1.6 E-Coli bacteria:

Escherichia coli are a Gram-negative rod-shaped bacterium (Figure 1.9) that lives in the digestive tracts of humans and animals. There are many

types of *E. coli* most of them harmless, but some types causes bloody diarrhea, anemia and kidney failure. *E. coli* infection caused by contact with feces, or stool, of humans or animals [36- 38].

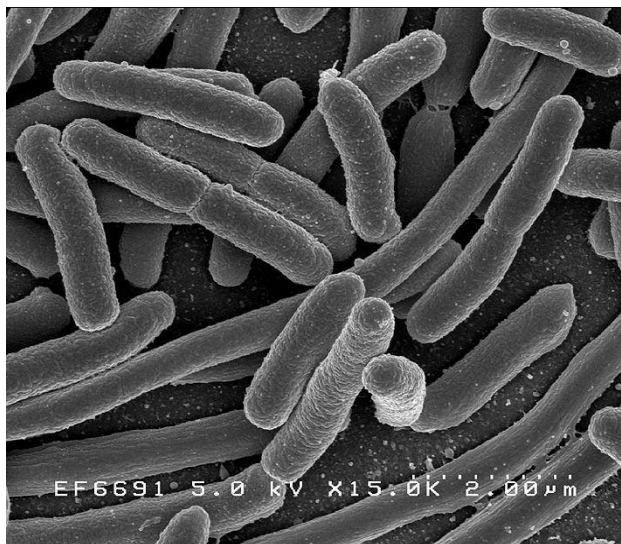


Figure 1.9: E-Coli bacteria [36].

1.7 Staphylococcus aureus:

S. aureus is a facultatively anaerobic Gram-positive coccus, which appears as grape-like clusters when viewed through a microscope (Figure 1.10). Staphylococci can be found normally in the nose and on the skin, and in the majority of cases the bacteria do not cause disease. However, damage to the skin or other injury may allow the bacteria to overcome the natural protective mechanisms of the body, leading to infection [39-41].

E-coli and *Staphylococcus aureus* bacteria have been chosen here as model bacteria to be photodegraded using TiO_2 /anthocyanin catalyst systems.

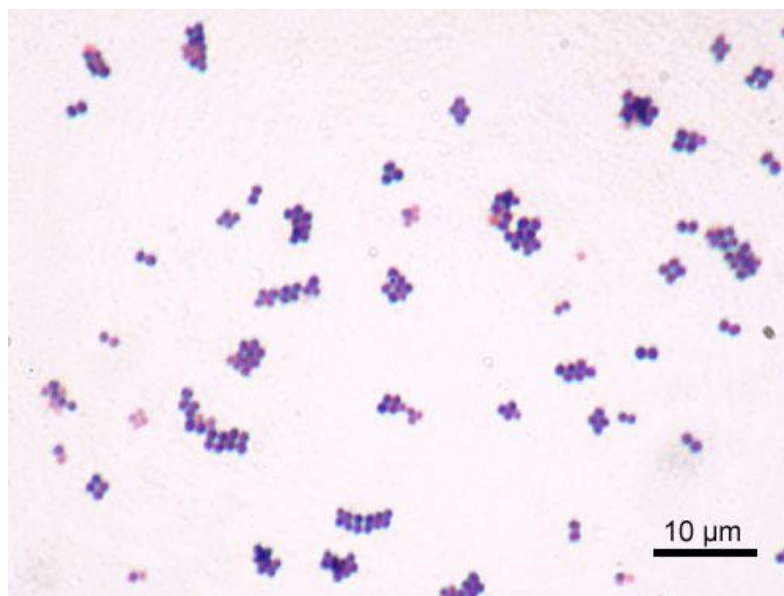


Figure 1.10: Gram stain of *S. aureus* cells [39].

1.8 Objectives:

- 1- Preparation of nano-particles of TiO_2 from TiCl_3
- 2- Supporting anthocyanin molecules onto nano- TiO_2 particles. Anthocyanin molecules (taken from Karkade) will be used as sensitizers for the TiO_2 particles.
- 3- Supporting TiO_2 on AC (activated carbon) then attaching the anthocyanin dye molecules to the TiO_2 .
- 4- Using TiO_2 /anthocyanin system as dye-sensitized semiconductor in solar degradation of water contaminants (bacteria and phenazopyridine).
- 5- Study kinetics of the photodegradation reaction

Chapter Two

Experimental

2.1 Material and chemicals:

TiCl₃ was purchased from Riedel-de Haen, as a 20% solution in HCl.

Ethanol, NaOH, HCl and AC (activated carbon) were purchased from Aldrich. Phenazopyridine hydrochloride was kindly donated from Berziet-Palestine Pharmaceutical Company. Hibiscus (Karkade) for anthocyanin natural dye extraction was purchased from local market.

2.2 Instruments:

2.2.1 UV/vis spectrophotometry:

A shimadzu UV-1601 spectrophotometer, equipped with thermal printer Model DPU-411-040, type 20BE, was used for electronic absorption spectra measurement.

2.2.2 Polarography:

Anodic stripping differential pulse polarography (ADPP) was conducted using drop mercury electrode (MDE 150) on a PC controlled polarograph (POL 150) to measure contaminant concentration during photo-degradation experiments.

2.2.3 Fluorescence Spectrophotometer:

A Perkin-Elmer LS50 Luminescence Spectrophotometer was used to measure emission fluorescence spectra for catalyst system.

Emission spectra was used to measure semiconductor catalyst band gap.

2.2.4 Lux-meter:

A Lux-meter (Lx-102 light meter) was used to measure the intensity of lamp radiation.

2.2.5 XRD:

Powder X-ray diffractometer (XRD, Rigacu, $k_{\alpha} = 1.54059 \text{ \AA}$, 298 K). The analysis was kindly performed by Mrs. J. Kim of ISAA Envirom. Consult. Co. Chugj-city, South Korea.

2.2.6 SEM:

Field emission-scanning electron microscopy (FE-SEM.JEOL JSM-6700F) with an energy dispersive X-ray spectrometer (EDS) analysis was kindly performed by Mrs. J. Kim of ISAA Envirom. Consult. Co. Chugj-city, South Korea.

2.3 Catalyst preparation

2.3.1 Preparation of TiO₂ powder:

TiCl₃ original solution (50 ml) was placed in a 250 mL conical flask. Then 100 ml of NaOH (2.5 molar) was added drop-wise with continuous stirring until the mixture became white in color. The resulting TiO₂ powder was decanted and washed with water 2-3 times. The powder was then separated from the mixture using a centrifuge (speed 5000 round per minute). The isolated powder was left to dry at room temperature [42]. The yield was nearly higher than 90%.

2.3.2 Extraction of anthocyanine dye:

Commercial Karkade dried flowers (30 g) were crushed and soaked in a 500 ml Erlenmeyer flask with 300 ml of ethanol with gentle magnetic stirring at room temperature for 1 hr. The solution was then filtered and stored into a dark color glass bottle.

2.3.3 Preparation of TiO₂/Anthocyanin

TiO₂ (8.0 g), prepared as described earlier, was refluxed for half an hour with 100 ml of anthocyanin ethanolic extract. The mixture was then left to cool, it was chilled in ice for 15 minutes. The TiO₂/Anthocyanin was suction-filtered through sintered glass, and the solid powder was collected

and washed with cold water. The solid was then dried in air and kept in the dark for further use.

2.3.4 Preparation of AC/TiO₂/Anthocyanin:

The AC/TiO₂/Anthocyanine system was prepared as follows: The white TiO₂ particle suspension (150 mL, containing about 8.0 g TiO₂), prepared as mentioned previously, was mixed with activated carbon (2.00 g) and stirred for one hour. The mixture was then filtered and dried in oven at 130°C. Anthocyanin alcoholic extract (100 mL) was added to the resulting dried TiO₂/AC powder (~10.00 g) and stirred for one hour. The mixture was then filtered, and the solid left to dry at room temperature. The resulting AC/TiO₂/Anthocyanin system was stored in the dark for further use. The amounts of anthocyanin (per gram solid) adsorbed by TiO₂ and AC/ TiO₂ were similar. This is because the activated carbon surface was not exposed to anthocyanin dye during mixing.

2.3.5 Stock solution preparation:

Three stock solutions were needed for photocatalytic experiment:

- contaminant stock solution (100 ppm) was prepared by dissolving phenazopyridine (0.10 g) in distilled water. The resulting solution was then diluted to 1.00 L with distilled water, and kept in the dark.

- Dilute solutions (0.05M) of both HCl and NaOH were prepared for the purpose of controlling the pH in the catalytic reaction mixtures.

2.4 Calibration curve:

Six known concentrations of phenazopyridin (5, 10, 15, 20, 25, and 30 ppm) were prepared and measured by polarography.

2.5.1 Photo-Catalytic Experiments:

Catalytic experiments were conducted in a 100 mL magnetically stirred thermostated beaker. The out-side walls of the beaker was covered with aluminum foil to reflect back astray radiations. The glass beaker was dipped in controlled temperature water bath. Aqueous reaction mixtures (50 mL) of known concentrations of contaminant and catalyst were placed in the beaker. The pH was controlled as desired by adding drops of NaOH or HCl dilute solutions. Direct visible irradiation using a solar simulator halogen spot lamp (1300 Lux, $0.0001898\text{W}/\text{cm}^2$) was applied vertically to the photo-catalytic mixture surface. The change in contaminant concentration was measured with time. Small aliquots of solution were syringed out from reaction vessel at different reaction times then centrifuged (5000 round/minute for 5 minutes). Five drops from this solution were added to 5 ml Britton – Robinson buffer at pH 8 [35] then measured by polarography.

2.5.2 Control experiments:

- In the absence of any catalyst, contaminant solution (50 ml) was placed in the reactor under visible light with stirring for 100 min. The absorption was measured before and after exposure to light. The contaminant concentration did not decrease under visible light with time. This means that the contaminant did not photo-degrade in the absence of catalysts.

- In the dark, 50 ml of contaminant were stirred with AC/ TiO₂ /anthocyanin (0.1 g) catalyst for 120 min. The absorption spectra was measured with time. The contaminant concentration continued to decrease until it reached a constant equilibrium value after ~120 min. The contaminant concentration loss was due to adsorption onto the AC/TiO₂/Anthocyanin. To account for adsorbed contaminant in later photocatalytic reaction experiments, the mixture of contaminant and catalyst was stirred in the dark for at least 120 min, before exposure to light. The reaction profiles were then monitored the moment the mixture was exposed to light.

2.6 Photocatalytic Degradation of Phenazopyridin:

Effects of pH, temperature, catalyst concentration and contaminant concentration, on rate of photo-degradation reaction, were all studied.

2.6.1 Effect of pH:

The degradation rate was studied at different pH values 3, 5, 7, and 9.

The samples were prepared as mentioned previously. The pH was controlled by adding drops of NaOH and HCl. Aliquots were syringed out of the reaction vessel every 25 min then centrifuged and measured by polygraphy.

2.6.2 Effect of contaminant concentration:

Three different concentrations of phenazopyridine were prepared (30, 35 and 40 ppm). Then 50 ml of each concentration were placed in the catalytic reactors. As mentioned above, the concentration of phenazopyridine was measured every 25 min for each concentration.

2.6.3 Effect of temperature:

The photo-degradation rate of phenazopyridine at different temperatures (15, 25, 35, 45C^o) was studied at constant pH, constant phenazopyridine and catalyst concentration the photo-catalytic experiments and measurements were done as mentioned above.

2.6.4 Effect of catalyst concentration:

Different amounts of catalyst were used (0.05, 0.075, and 0.15 g) to study the effect of catalyst concentration.

2.7 Photocatalytic Degradation of Bacteria:

2.7.1 Material and equipment

Two different types of pathogenic microorganisms of undesignated strain or serotype were isolated from clinical specimens. *E coli* were isolated from patient with urinary tract infection, while *Staphylococcus aureus* was isolated from patients with wound infection. The isolates were identified according to standard diagnostic methods. The inoculum of microorganisms was prepared using 4 h cultured nutrient broth and suspensions were adjusted to 0.5 McFarland standard turbidity. All work with microorganisms was done under sterile conditions.

2.7.2 Photo-Catalytic Experiments:

Four 100 ml-beakers, numbered from 1 to 4, were prepared with 50 ml of sterile nutrient broth and final concentration of bacterial suspensions 5×10^5 CFU/ ml.

- Beaker no. 1 is control
- Beaker no. 2 is control in dark
- Beaker no. 3 treated with of TiO_2
- Beaker no. 3 treated with TiO_2 / anthocyanin (0.10g)

With exception of beaker No. 2, the beakers were exposed to light for 90 min with continuous mixing and the temperature was maintained from 25-

30°C. The Number of bacteria in each beaker was quantitatively determined using plate count method

Chapter Three

Results and Discussion

3.1. Characterization results:

3.1.1 X-ray diffraction (XRD):

XRD patterns were measured for TiO_2 , $\text{TiO}_2/\text{anthocyanin}$, and $\text{AC}/\text{TiO}_2/\text{anthocyanin}$ as shown in (Figure 3.1):

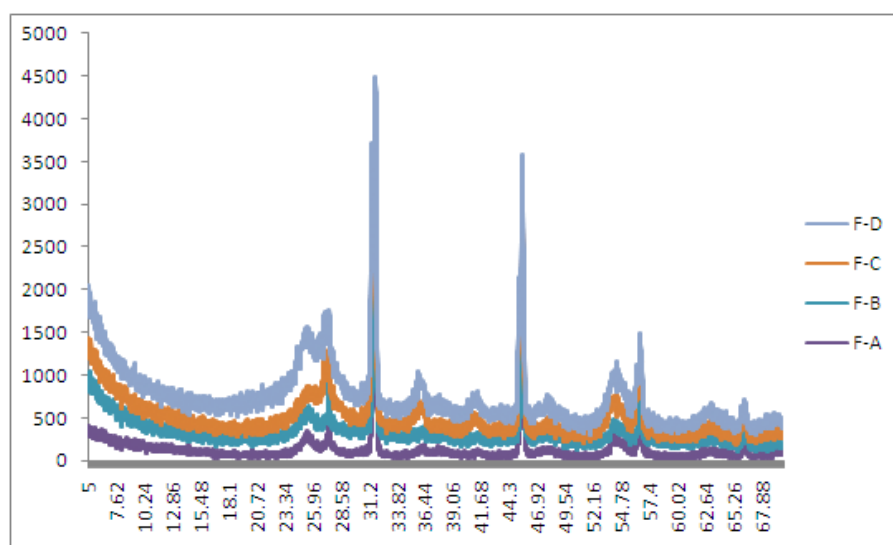


Figure 3.1: X-ray diffraction pattern for A: TiO_2 , B: $\text{TiO}_2/\text{anthocyanin}$, C: $\text{TiO}_2/\text{anthocyanin}/\text{AC}$

The XRD results were compared to earlier literature, as summarized in Table (3.1) [43-44]

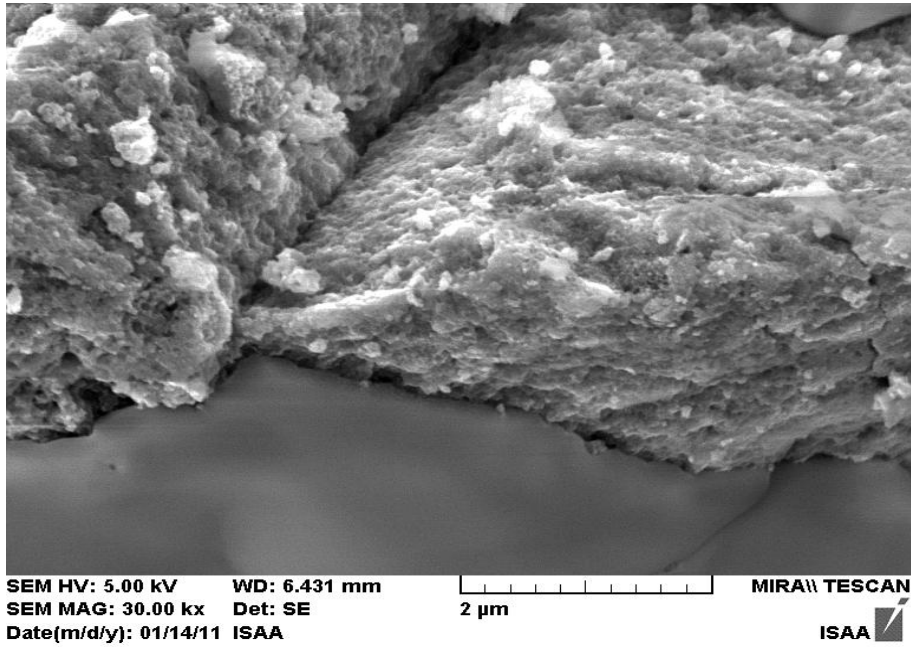
Table 3.1: XRD data for prepared TiO₂ compared with anatase and rutile

Observed 2 θ	Anatase (planes)	Rutile (planes)
25.3	(101)	
27.6		(110)
36		(101)
38.5	(004)	
41.2		(111)
48	(200)	
54.7	(211)	(211)
63	(118)	

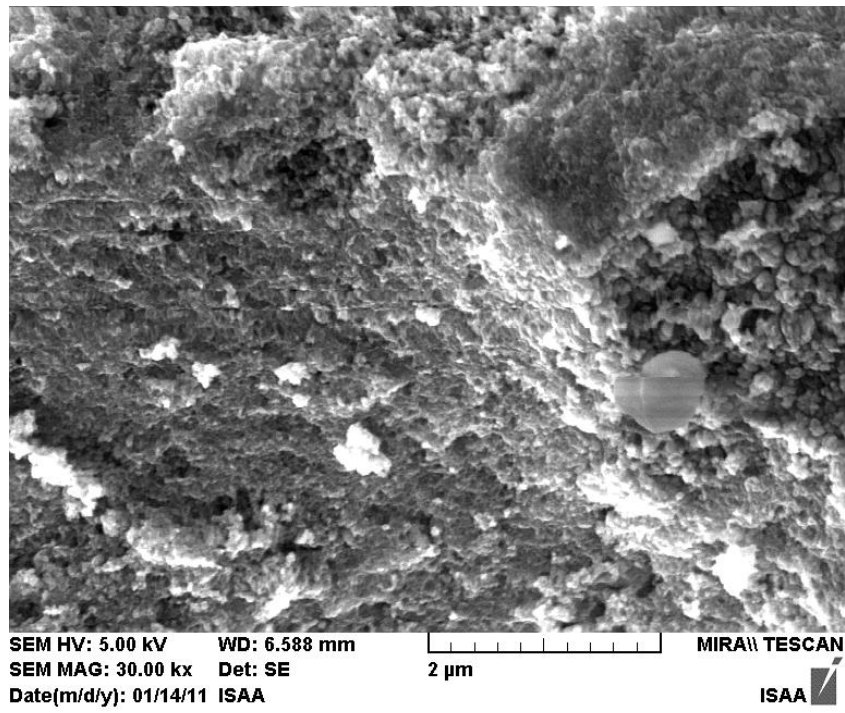
The XRD patterns showed that the prepared TiO₂ powder was a mixture of Rutile and Anatase forms. The three peaks at $2\theta = 31, 45.5, 57$ belong to NaCl impurity, as evidenced from literature [45- 46]. The impurity resulted from the reaction between HCl (from TiCl₃) and NaOH.

3.1.2 Scanning Electron Microscopy (SEM):

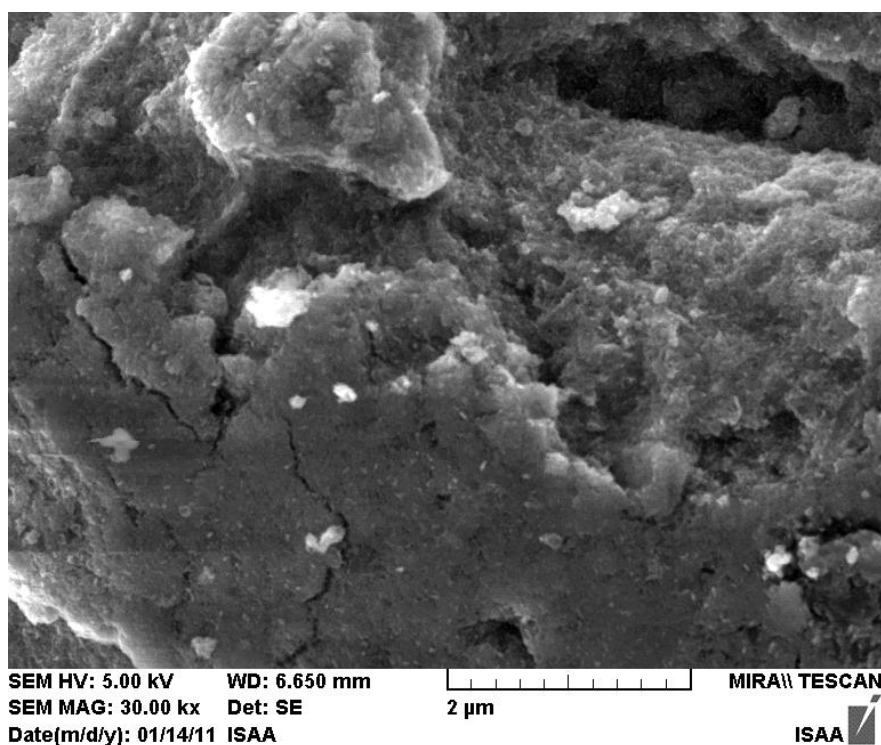
SEM pictures were made to investigate the surface morphology of the prepared TiO₂, TiO₂/anthocyanin and AC/ TiO₂/anthocyanin, as shown in (Figure 3.2). The Figure shows that the TiO₂ particle size was in the nano-scale, (~30 nm). The unsupported TiO₂ particles have more porous surface than their AC-supported counterparts. The attached anthocyanin does not have noticeable effects on solid surface textures. This means that the dye exists at the surface in the form of molecules rather than coagulates of dyes.



A



B



C

Figure 3.2: SEM images for A) TiO_2 , B) TiO_2 /anthocyanin, C) TiO_2 /anthocyanin/AC

3.1.3 TiO_2 photoluminescence spectra:

Photoluminescence emission spectra were studied for both commercial and prepared TiO_2 samples. Excitation was conducted using 360 nm wavelength. The observed emission peaks occurred at 415 nm for prepared TiO_2 , and 416 nm for commercial anatase TiO_2 (Figure 3.3):

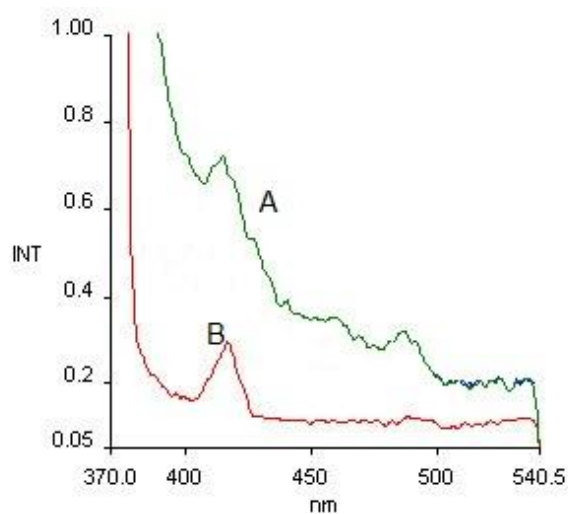
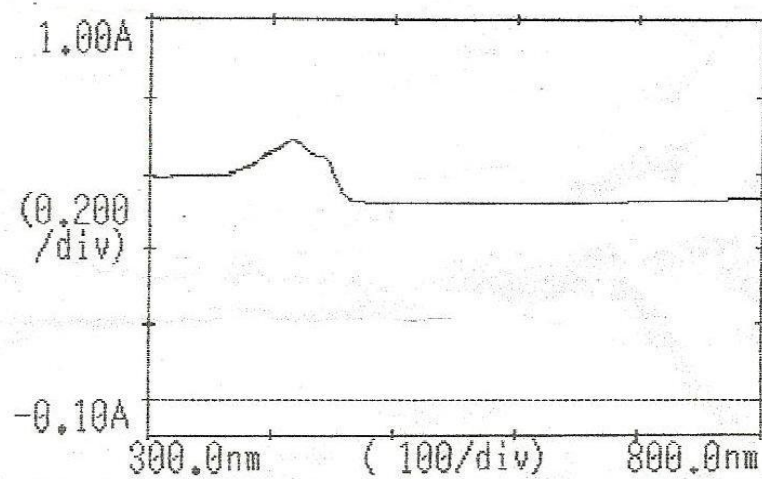


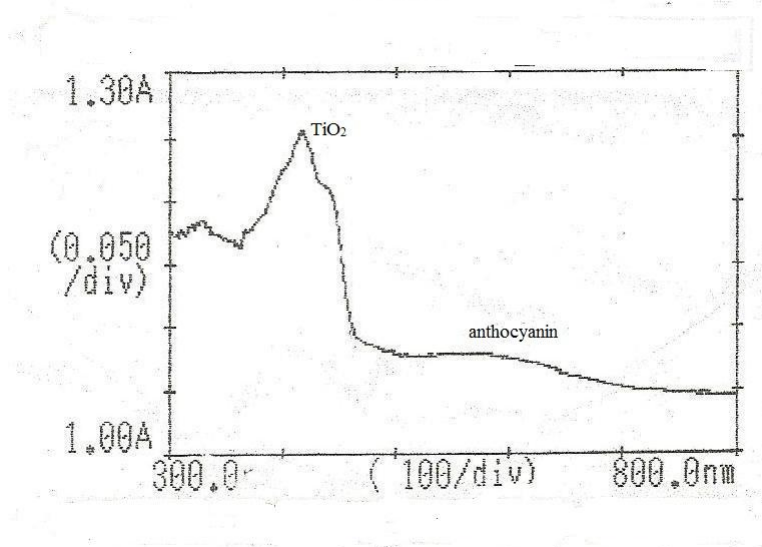
Figure 3.3: Photoluminescence spectra measured for TiO₂: a) prepared, and b) commercial samples, excitation wavelength was 360 nm.

3.1.4 UV- Visible Characterization:

UV-Visible spectra were measured for TiO₂, and TiO₂/anthocyanin systems, (Figure 3.4). Spectrum A for TiO₂ showed maximum absorbance at 420 nm showing a band gap about 3 eV for a rutile structure of TiO₂. Spectrum B for TiO₂/anthocyanin showed two peaks the first at 420 nm for TiO₂, and the second for anthocyanin dye at 580 nm. The band differs from that of anthocyanin dyes measured in solution (Figure 3.5) which means that the dye is chemically attached to TiO₂ in a chemisorptions pattern. The results confirm the presence of anthocyanin in the TiO₂/anthocyanin system.



(a)



(b)

Figure3.4: Solid state electronic absorption spectra measured for (a): TiO_2 , (b): $\text{TiO}_2/\text{anthocyanin}$

3.1.5. anthocyanin characterization :

- UV- Visible Characterization :

The UV-visible spectra shows the maximum wavelength absorbance was at ~ 540 nm Figure (3.5).

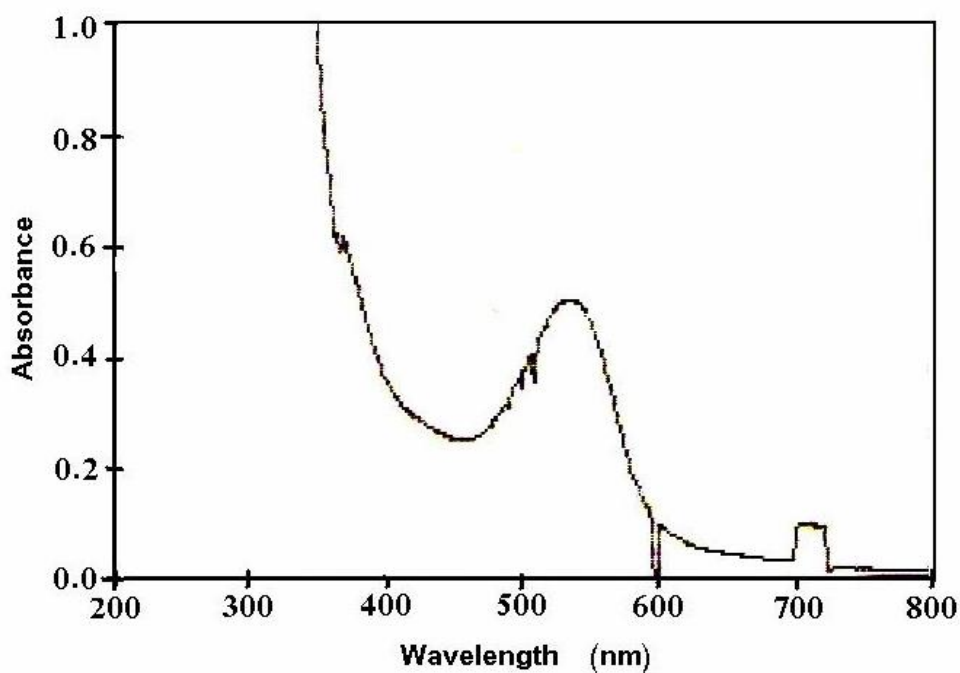


Figure 3.5: Solid state electronic absorption spectra measured for anthocyanin dye.

-TLC characterization:

Thin layer chromatography measured for the extracted anthocyanin dye in methanol shows that the solution includes only one component, Figure (3.6). Therefore, TLC is consistent with electronic absorption spectra, and the resulting anthocyanin solution involves only one dye compound.



Figure 3.6: TLC measured for one anthocyanin solution, showing only one component for extracted dyes.

3.2. Photocatalytic Degradation of Phenazopyridin:

TiO₂ and TiO₂/anthocyanin systems were first used as catalysts for photodegradation of phenazopyridine. Due to their highly porous surfaces, neither system was suitable to be used as photo-catalyst. Both systems adsorbed relatively high amounts of contaminant, due to high porosity. While using 50.0 mL solutions, of 70 ppm contaminant concentrations, all contaminant molecules disappeared onto the solid catalyst (0.10 g) in less than 120 min.

On the other hand, the AC/ TiO₂/anthocyanin system was less porous than the above mentioned ones. This was evidenced from SEM images. This explains why the supported TiO₂ system adsorbed less contaminant (25 ppm per 0.1 g) than the unsupported TiO₂ systems. For these reasons photo-

degradation of phenazopyridin was conducted using the TiO_2 /anthocyanin/AC system unless otherwise stated.

3.2.1 Calibration Curve:

A calibration curve was used to measure concentration of remaining phenazopyridine in solution with time. By measuring the current of the sample, the contaminant concentration was deduced from the calibration curve (Figure 3.7).

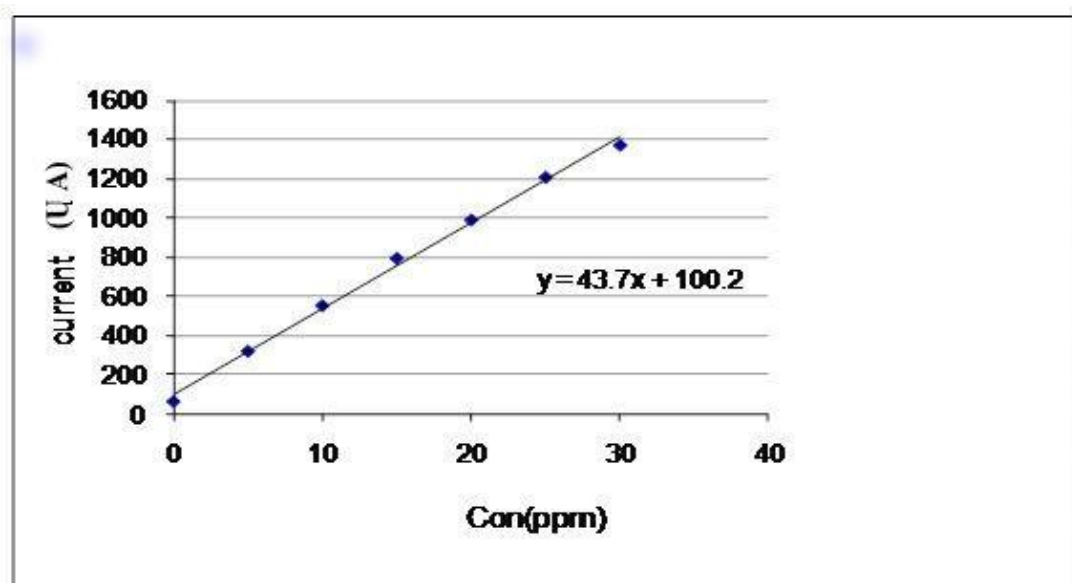


Figure 3.7: Polarography calibration curve showing current vs. contaminant concentration.

3.2.2. Control experiment results:

A number of control experiments were conducted to confirm the role of AC/ TiO_2 /anthocyanin system as catalyst for photodegradation of phenazopyridin.

- Experiments without catalyst under solar simulator radiation:

When contaminant solution was irradiated in the absence of any catalyst, no decrease in contaminant concentration was observed for more than 120 min. This means that the contaminant did not degrade in the absence of catalysts.

- Experiments with AC/TiO₂/Anthocyanin in dark:

Effect of adding AC/ TiO₂/anthocyanin system to contaminant solutions (40 ppm) in the absence of light was studied. As a result, contaminant concentration continued to decrease until it reached a constant equilibrium value (~15 ppm) after ~120 min. Such contaminant concentration loss is due to adsorption onto the AC/TiO₂/Anthocyanin. Such observations were taken into consideration when using the TiO₂/anthocyanin/AC system in photodegradation experiments of phenazopyridin.

3.2.3 Photo-catalytic experiment results:

To account for adsorbed contaminant in photo-catalytic reaction experiments, the mixture of contaminant and catalyst was stirred in the dark for at least 120 min, before exposure to light. The catalytic reaction profiles were then monitored the moment the mixture was exposed to light.

The phenazopyridin photodegradation reaction was studied using AC/TiO₂/anthocyanin system in water. Effects of different reaction parameters, such as pH, temperature, catalyst concentration and

contaminant concentration, on rate of photo-degradation reaction, were all studied.

3.2.3.1 Effect of pH:

The pH value is an important variable in photocatalytic degradation reactions. That is because it influences the surface electric charge of TiO₂ catalyst [47]. The point of zero charge of TiO₂ (pH_{pzc}) is close to pH 6.8. At values higher than pH_{pzc}, the surface of TiO₂ becomes negatively charged as follows:



When the value is lower than pH_{pzc} the surface of TiO₂ becomes positively charged as follows [48]:



Anthocyanin is more stable in acidic media than in alkaline media. It has four structures in aqueous media as shown in Figure (3.8)

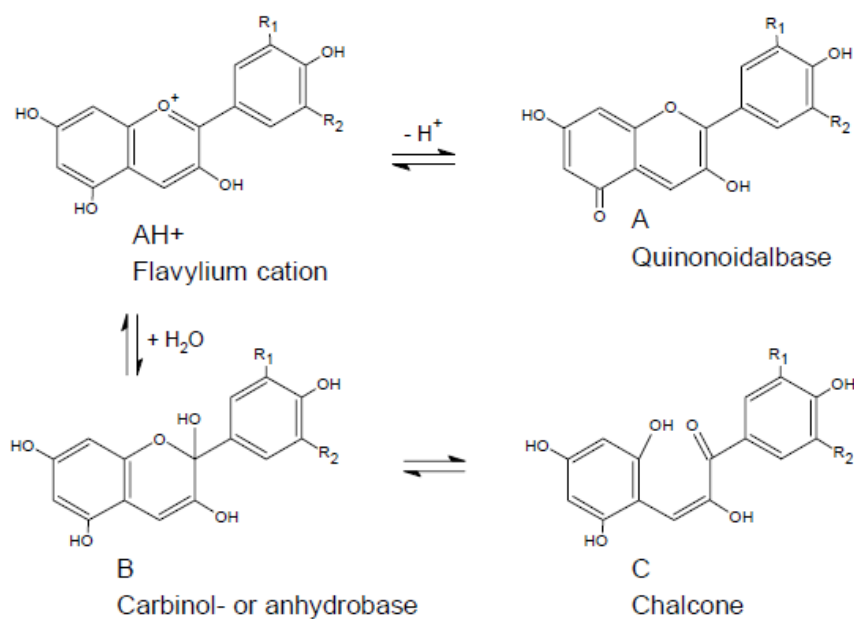


Figure 3.8: The main four equilibrium forms of anthocyanin existing in aqueous media. [49]

In acidic media (pH 0.5) the red flavylium cation is the only equilibrium species. When pH increased the intensity of red color decreased due to decreased concentration of flavylium cation.

When anthocyanin bonds to TiO_2 , its stability increases even with higher pH [49]. This adds to the credibility of using anthocyanin sensitizers.

Phenazopyridine degradation was studied at different pH values, as shown in (Figure 3.9).

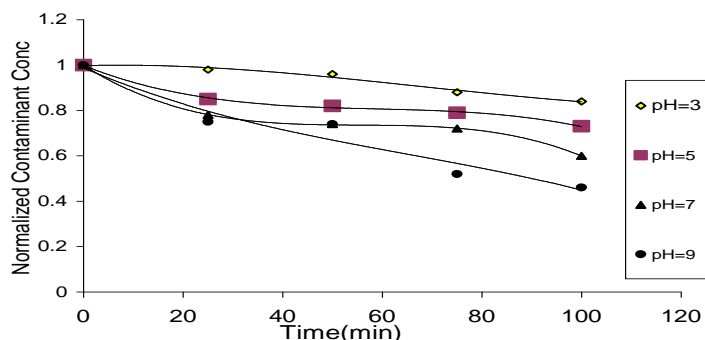


Figure 3.9: Effect of pH on phenazopyridine photodegradation rate. All measurements were made at room temperature in aqueous solutions (50 mL) using 40 ppm starting contaminant solution, and AC/TiO₂/ anthocyanin (0.10 g).

Table (3.2) summarizes the results of Figure (3.6). From the Table and the Figure, the values for degradation percent, TN, TF and QY were all increased with higher pH value. This means that the catalyst efficiency is higher at higher pH values. This is in consistent with literature, where some phtodegradation reactions became faster at higher pH [50]. Contrary to these results, some photodegradation reactions became slower at higher Ph[51-52].

Table 3.2: Values of %degradation, turnover number (TN), turnover frequency (TF) and quantum yield (QY) measured for phenazopyridin degradation after 100 min.

pH	% degradation	TN	TF (min ⁻¹)	QY (molecule/photon)
3	15	4.8×10^{-4}	4.8×10^{-6}	43.7×10^{-4}
5	26	7.89×10^{-4}	7.89×10^{-6}	0.0071
7	40	10.026×10^{-4}	10.026×10^{-6}	0.0073
9	54	16×10^{-4}	16×10^{-6}	0.0145

Where: TN = number of moles of reacted contaminant/number of moles of TiO₂ catalyst.

Number of contaminant moles reacted = (Initial concentration in ppm × percent of degradation × 50 / 1000000) / Mwt phenazopyridine (213.239)

Percent Degradation = [(Initial Conc. – Final Conc.) / initial conc.] × 100%

Moles of catalyst (TiO₂) = Wt / MM = 0.1 / 79.866 × 3/4 = 1.25×10^{-3} mol

Turnover frequency = TN / time (100 minute)

QY = number of contaminant molecules reacted / total number of photons used

E (J) = Incident power per unit area X Total area or incident power X Exposure time in second

= [(0.000189 W/cm²) × 21.6 cm²] × [100 × 60 second] = 24.6 J

Assuming average wavelength of incident light is 500 nm, then:

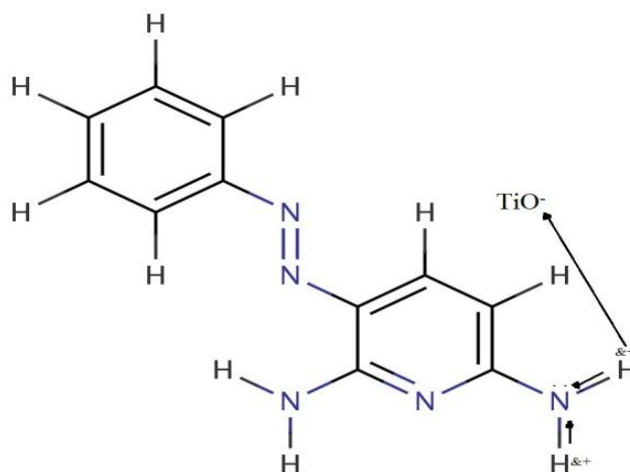
$\nu = c/\lambda = 3 \times 10^8 \text{ ms}^{-1} / 500 \times 10^{-9} \text{ m} = 6 \times 10^{14} \text{ s}^{-1}$

And from Planks equation, E (J) = $nh\nu$

$n = E/h\nu = 24.6 / (6 \times 10^{14} \times 6.62 \times 10^{-34}) = 0.62 \times 10^{20}$ photons

The discussions presented above explain effect of pH. At lower pH values, the TiO₂ surface is positively charged, whereas at higher pH the surface is negatively charged. On the other hand, at lower pH values, the contaminant phenazopyridin gains positive charges [48-50]. As a base, phenazopyridine retains its neutral charge at higher pH values. This explains the effect of pH on activity. At lower pH values, both TiO₂ and phenazopyridine are positively charged, which lowers adsorption of the latter onto the former. At higher pH values, TiO₂ surface carries negative charge. This negative

charge attracts the partial positive charges present onto H-atoms of the amine group of neutral phenazopyridin. These discussions are explained in Scheme 1.1. As adsorption increases, with higher pH, photodegradation catalyst efficiency is expected to increase.



Scheme 3.1

3.3.3.2 Effect of contaminant concentration:

Effect of contaminant concentration on phenazopyridin photodegradation rate was studied. Different contaminant nominal concentrations (30, 35 and 40 ppm) were used. It should be noted that after the catalytic mixture was left in the dark for 120 min, contaminant adsorption occurred. After equilibrium was reached, the initial remaining contaminant concentrations, before photodegradation started were measured to be 10, 13 and 16 ppm. (Figure 3.10) shows reaction profiles for normalized remaining contaminant concentrations with time.

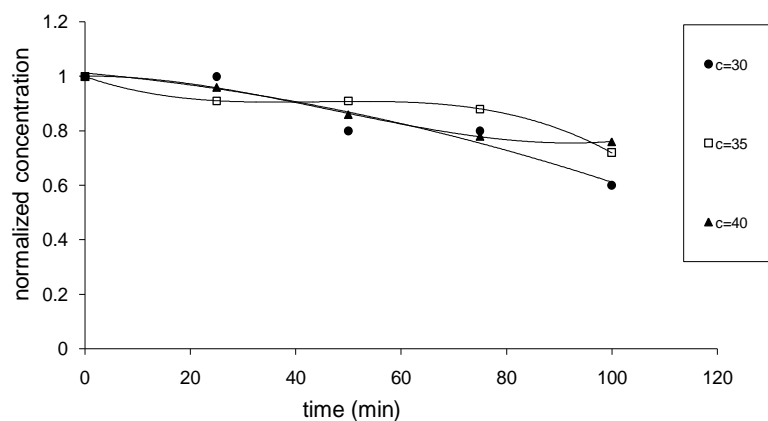


Figure 3.10: Effect of contaminant concentration on %photo-degradation at room temperature and pH 3.5.

The data presented in (Figure 3.7) are summarized in Table (3.3). Values of TN, TF and QY were recalculated as mentioned above, and are shown in the Table.

Table 3.3: Values of TN, TF, QY, and %phenazopyridine degradation for catalytic runs using different contaminant concentration.

Nominal concentration	Initial concentration	Final concentration	% degradation	Turnover number	Turnover frequency	Quantum yield
30	9.7	6.5	33	8×10^{-4}	8×10^{-6}	0.0058
35	12.5	9	28	8.86×10^{-4}	8.86×10^{-6}	0.0078
40	15.6	12	23	8.96×10^{-4}	8.96×10^{-6}	0.0081

Table (3.3) shows that phenazopyridine photo-degradation reaction percentage decreased as contaminant initial concentration increased. This should not be an indication of catalyst efficiency. Values of quantum yield increased with increasing contaminant concentration. This indicates that catalyst efficiency increases with increasing contaminant concentration. Moreover, the values of catalyst TN and TF also increased with higher contaminant concentration. Collectively, the results indicate that the catalyst efficiency is higher with higher initial contaminant concentration. Our results are consistent with earlier studies using ZnO catalyst [53].

Contrary to these results, Jun Yao used degradation percentage for studying effect of contaminant concentration on catalyst efficiency [47]. This should not be the case, because percentage may not necessarily tell about efficiency, especially when using different contaminant concentrations.

3.2.3.3 The effect of temperature:

Generally speaking, literature shows that photocatalysis processes are not temperature dependent [51, 54]. Effect of temperature on phenazopyridin photo-degradation rate was studied here. Different temperatures (15, 25, 35 and 45°C) were used. The results are shown in (Figure 3.11) and summarized in Table (3.4). The Figure shows that the rate of photocatalytic degradation is not much affected with temperature, with little increase as temperature is increased.

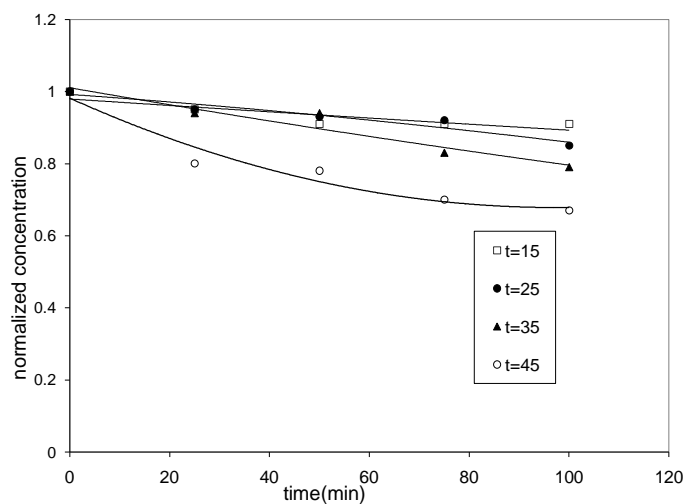


Figure 3.11: Effect of temperature on phenazopyridine photo-degradation rate

From Table (3.4), values of QY, TN, TF and the percent of degradation slightly increased with increasing the temperature.

Table 3.4: Values of TN, TF, QY and %phenazopyridine degradation for catalytic runs using different temperatures.

Temperature	% degradation	TN	TF	QY
15	8.5	2.98×10^{-4}	2.98×10^{-6}	0.0027
25	14	4.93×10^{-4}	4.93×10^{-6}	0.0045
35	20	7.46×10^{-4}	7.46×10^{-6}	0.0068
45	32.5	11.2×10^{-4}	11.2×10^{-6}	0.0102

Value of activation energy (E_{act}) was calculated using plots of \ln (initial rate) vs. $(1/T)$, as shown below. The value of E_{act} was relatively small (19 kJ/mol). This explains the observed small effect of temperature on reaction rate, as shown in Table (3.4). The results observed here are thus consistent with earlier literature reports [51].

Calculation the activation energy E_{act} :

(Figure 3.12) shows the relation between phenazopyridine concentration and time at each temperature. From the slope of each curve at initial concentration we calculate the initial rate of reaction at each temperature was measured.

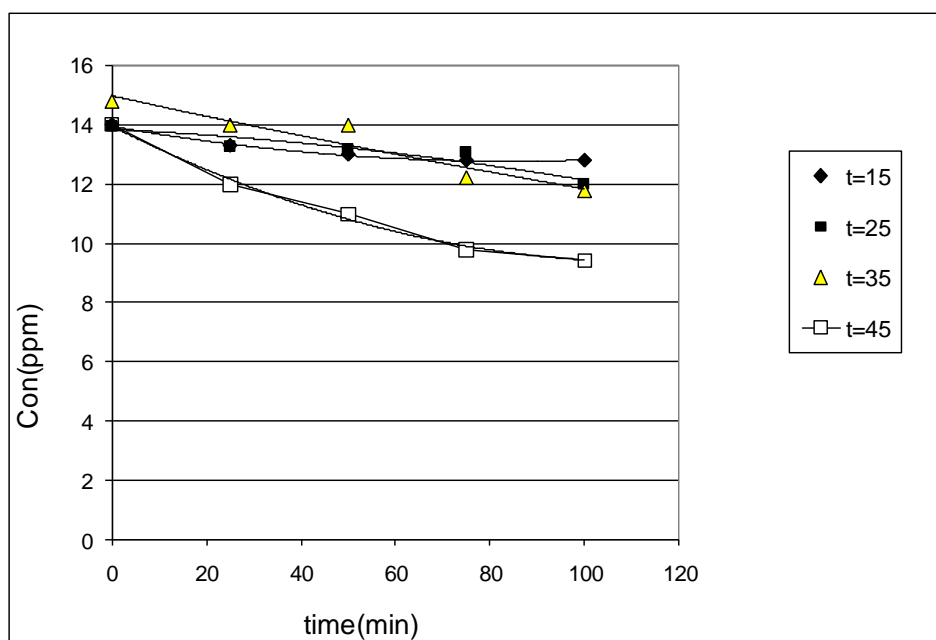


Figure 3.12: Reaction profiles showing contaminant concentration with time at different temperatures.

Assuming constant initial contaminant concentration then

$$\text{Initial rate} = k [\text{contaminant}]^n$$

$$\text{Its known that } k = Ae^{-E_a/RT}$$

Where A is Arhenius constant

E_{act} is activation energy (J/mol)

R is gas constant (8.314 J/mol K)

T is temperature (in Kelvins)

Using natural logarithms then:

$$\ln k = -E_{act}/RT + \ln A$$

Based on data of Figure 3.12 and Table (3.5), values of $\ln k$ were plotted vs. values of $(1/T)$ as shown in Figure (3.13). A linear relation was observed, where the slope equals $(-E_{act}/RT)$ and the intercept equals $\ln(A)$. From value of slope and knowing $R=8.314\text{J/mol K}$, the value of E_{act} was calculated as

$$\text{Slope} = -2321$$

$$\text{Slope} = -E_{act}/R$$

$$E_{act} = 19.3 \text{ kJ/mol}$$

Table (3.5): Values of $\ln(\text{rate})$ vs. $1/T$ for phenazopyridine photodegradation experiments.

$1/T$	$\ln \text{ rate}$
0.00347	-22.6
0.00355	-22.6
0.00324	-22
0.003144	-21.7

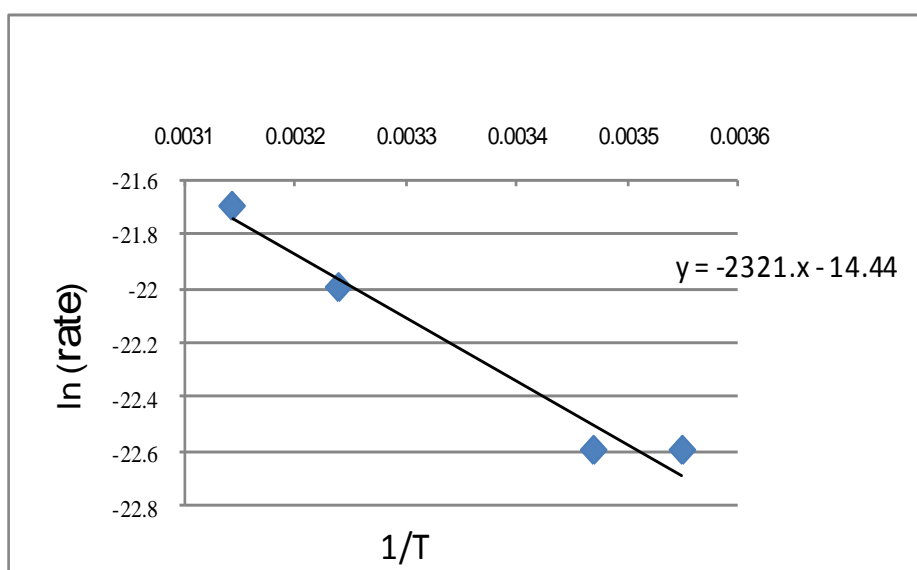


Figure 3.13: Plots of $\ln(\text{rate})$ versus $1/T$ for photo-degradation of phenazopyridine.

3.2.3.4 Effect of catalyst concentration:

The effect of catalyst concentration on photo-degradation reaction rate was studied using different amounts of AC/TiO₂/anthocyanin catalyst, namely 0.05g, 0.075 g, 0.15 g. The relation between catalyst concentration and photo-degradation rate was presented in (Figure 3.14):

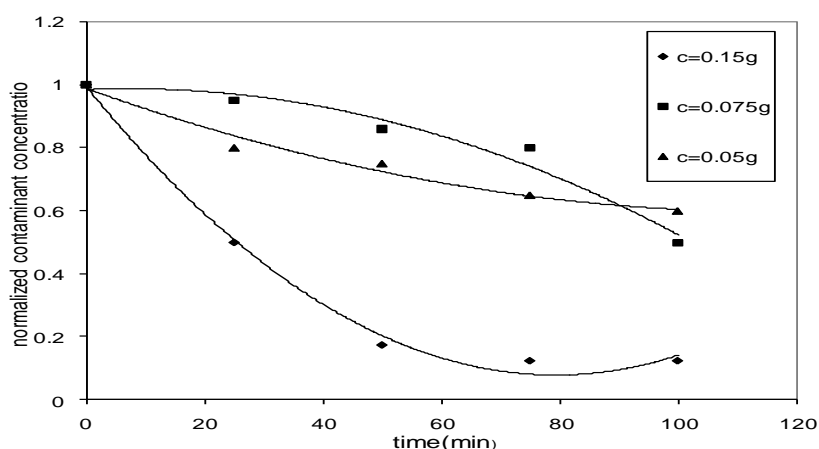


Figure 3.14: Effect of catalyst concentration at room temperature, pH 3.5

As shown in (Figure 3.14) increasing the catalyst concentration increased the rate of photo-degradation. This is understandable, as number of catalytically active sites increases with catalyst concentration.

Earlier literature shows that catalyst effect on efficiency is also affected by contaminant concentration itself [51, 54]. With higher contaminant concentration, catalyst efficiency increases with higher catalyst concentration. With lower contaminant concentration, the efficiency increases with higher catalyst concentration until a maximum value is observed. After that, efficiency decreases with higher catalyst concentration. This resembled earlier reports. When the concentration of contaminant increased availability of excess active sites outweighs the diminishing photoactivated volume, and increased the rate of degradation

[51, 54]. Values of percent degradation, turnover number, turnover frequency and quantum yield are summarized in Table (3.6):

Table 3.6: Values of, TN, TF, QY and %phenazopyridine degradation for catalytic runs with different catalyst concentration.

Catalyst wt	% degradation	Turnover number	Turnover frequency	Quantum yield
0.05 g	28.5	4.93×10^{-4}	4.93×10^{-6}	0.0045
0.075 g	50	5.44×10^{-4}	5.44×10^{-6}	0.0049
0.15 g	87.5	8.86×10^{-4}	8.86×10^{-6}	0.0079

3.3 Photodegradation of Bacteria:

3.3.1 *E coli* photodegradation

Our preliminary results show that after 90 minute of treatment the percent of photodegradation is 22% Table, (Figure 3.15).

Table 3.7: *E-coli* counted number under different experimental conditions

Beaker	No. of Bacteria
Control	13.3×10^5 CFU/ ml
Control in dark	5×10^5 CFU/ ml
Bacteria with 0.1g of TiO ₂	12.5×10^5 CFU/ ml
Bacteria with 0.1g of TiO ₂ / anthocyanin (0.1g)	10.4×10^5 CFU/ ml

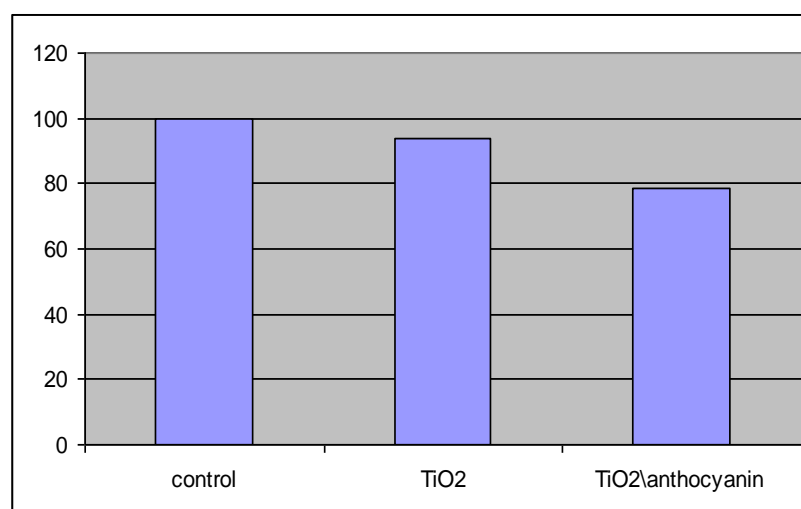


Figure 3.15: Percent of photodegradation of E-coli bacteria using TiO₂ and TiO₂/anthocyanin

3.3.2 *Staphylococcus aureus* photodegradation

Our preliminary studies show that after 90 minute of treatment there no noticeable effect of catalyst, but when we increase the catalyst concentration (0.15g) the percent of photodegradation was 17% Table 3.8, (Figure 3.16) this is may be due to that Staph. is gram positive bacteria which has a very thick cell wall.

Table 3.8: *Staphylococcus aureus* counted number under different experimental conditions.

Beaker	No. of Bacteria
Control	12.5×10^5 CFU/ ml
Control in dark	5×10^5 CFU/ ml
Bacteria with 0.15g of TiO ₂	12.9×10^5 CFU/ ml
Bacteria with 0.15g of TiO ₂ / anthocyanin	10.4×10^5 CFU/ ml

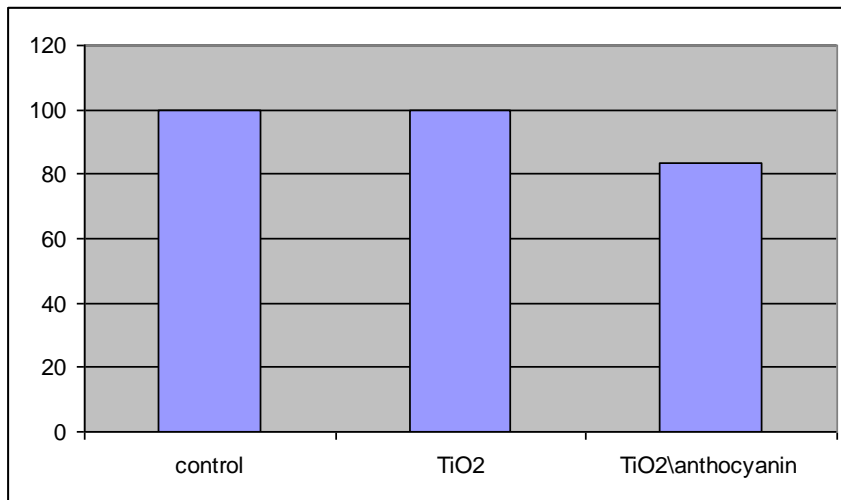


Figure 3.16: Percent of photodegradation of *Staphylococcus aureus* bacteria using TiO₂ and TiO₂/ anthocyanin.

3.4 Conclusions:

- 1- The reaction between TiCl_3 and NaOH produced a mixture of anatase and rutile nano-particles of TiO_2
- 2- Phenazopyridine was photodegraded using TiO_2 /anthocyanin/AC catalyst system and halogen spot lamp.
- 3- The efficiency of the catalyst increased with increasing pH, temperature, catalyst concentration and contaminant concentration.
- 4- Preliminary screening study shows that the system efficiently catalyzed bacteria degradation.

3.5 Suggestions for further work:

- 1- Using semiconductors other than TiO_2
- 2- Using other types of natural dyes for semiconductor sensitization
- 3- More study for bacteria degradation using sensitized semiconductor and visible light, needs to be done
- 4- Study contaminant photodegradation in air and soil using TiO_2 /anthocyanin catalyst system and visible light.

REFERENCES

- [1] <http://www.laleva.cc/environment/water.html> (accessed 1/9/2010).
- [2] N. Lydakis-Simantiris, D. Riga, E. Katsivela, D. Mantzavinos, and N. P. Xekoukoulotakis. “**Disinfection of spring water and secondary treated municipal wastewater by TiO₂ photocatalysis**”. *Desalination*, **250**, (2010),**351**.
- [3] T. E. Schultz. “**Biological wastewater treatment** ”. *Chemical Engineering*, **1**, (2005), **44**.
- [4] http://en.wikipedia.org/wiki/Ultraviolet_germicidal_irradiation (accessed 15/9/2010).
- [5] http://en.wikipedia.org/wiki/Water_purification (accessed 10/9/2010).
- [6] <http://www.lenntech.com/water-purification-steps-faq.htm> (accessed 10/9/2010).
- [7] K. Wongcharee, V. Meeyoo, S. Chavadej. “**Dye-sensitized solar cell using natural dyes extracted from rosella and blue pea flowers**”. *Solar Energy Materials & Solar Cells*, **91**, (2007), **566**.
- [8] J. M. Herrmann, C. Duchamp, M. Karkmaz, Bui Thu Hoai, H. Lachheb, E. Puzenat, C. Guillard. “**Environmental green chemistry as defined by photocatalysis**”. *Journal of Hazardous Materials* **146**, (2007), **624**.

- [9] A.S. STASINAKIS. **“Use of selected advanced oxidation processes(AOPs) for wastewater treatment- a mini review”**. *Global NEST Journal*, **10**, (2008), **376**.
- [10] C. Comninellis, A. Kapalka, S. Malato, S. A Parsons, I. Poulios, and D. Mantzavinos. **“Perspective advanced oxidation processes for water treatment: advances and trends for R&D”**. *Journal of Chemical Technology and Biotechnology*, **83**, (2008), **769**.
- [11] J. J . Pignatello, D. Liu , and P. Huston. **“Evidence for an additional oxidant in the photoassisted fenton reaction”**.
Environ. Sci. Technol, **33**, (1999),**1832**.
- [12] J. Prousek. **“Fenton chemistry in biology and medicine”**. *Pure Applied Chemistry*, **79**, (2007), **2325**.
- [13] K. Rajalakshmi. **“Photocatalytic reduction of carbon dioxide in conjunction with decomposition of water on oxidesemiconductor surface”** M.Sc. Thesis, Department of Chemical Engineering Indian Institute of Technology, Madras, May, (2011), p. **1**.
- [14] A. L. Linsebigler, G. Lu, and John T. Yates, Jr. **“Photocatalysis on TiO₂ Surfaces: Principles, Mechanisms, and Selected Results”**. *Chem. Rev*, **95**, (1995), **735**.

- [15] A. Sobczyński, A. Dobosz. **“Water Purification by Photocatalysis on Semiconductors”**. *Polish Journal of Environmental Studies*, **10**, (2001),**195**.
- [16] http://en.wikipedia.org/wiki/Titanium_dioxide (accessed 20/9/2010).
- [17] <http://www.nl-nd.com/khome.nsf/383AD6EE9A5545i23852569070068954C/166081EB14EAFA428525690E004E6662?OpenDocument> (accessed 21/9/2010).
- [18] O. Carp, C. L. Huisman, and A. Reller. **“Photoinduced reactivity of titanium dioxide”**. *Progress in Solid State Chemistry* **32**, (2004), **33**.
- [19] <http://ruby.colorado.edu/~smyth/min/tio2.html> (accessed 21/9/2010).
- [20] S. S. Srinivasan, J. Wade, and E. K. Stefanakos. **“Visible light photocatalysis via CdS/TiO₂ nanocomposite materials”**. *Journal of Nanomaterials*, **2006**, (2006), **1**.
- [21] C.J. Philippopoulos and M. D Nikolaki. **“Photocatalytic processes on the oxidation of organic compounds in water”**. *New Trends in Technologies*, **9**, (2010),**89**.
- [22] <http://photochemistryportal.net/home/index.php/2009/09/30/metal-oxide-photocatalysis> (accessed 26/9/2010).

- [23] T. Kim, Y. Lee, K. Park, S. J. Kim and S.Y. Cho. **“A study of photocatalysis of TiO₂ coated onto chitosan beads and activated carbon”**. *Research on Chemical Intermediates*, **31**, (2005). **343**.
- [24] J. N. Bhakta, Y. Munekage. **“Degradation of antibiotics (trimethoprim and sulphamethoxazole) pollutants using UV and TiO₂ in aqueous medium”**. *Modern Applied Science*, **3**, (2009), **2**.
- [25] L. L. Costa, A. G. S. Prado. **“TiO₂ nanotubes as recyclable catalyst for efficient photocatalytic degradation of Indigo carmine dye”**. *Journal of Photochemistry and Photobiology A: Chemistry* **201**, (2009), **45**.
- [26] R. Kato, A. Furube, A. V. Barzykin, H. Arakawa, M. Tachiya. **“Kinetics and mechanism of electron injection and charge recombination in dye-sensitized nanocrystalline semiconductors”**. *Coordination Chemistry Reviews*, **248**, (2004), **1195**.
- [27] S. Meng, J. Ren, and Ef. Kaxiras. **“Natural dyes adsorbed on TiO₂ nanowire for photovoltaic applications: enhanced light absorption and Ultrafast electron injection”**. *Nano Letters*, **8**, (2008), **8**.
- [28] Y. Bessekhoud, D. Robert, J.V. Weber. **“Bi₂S₃/TiO₂ and CdS/TiO₂ heterojunctions as an available configuration for photocatalytic degradation of organic pollutant”**. *Journal of Photochemistry and Photobiology A: Chemistry* **163** (2004) **569**.

- [29] A. Zyoud, “**Nanoparticle CdS-Sensitized TiO₂ Catalysis for Photo-Degradation of Water Organic Contaminants: Feasibility Assessment and Natural-Dye Alternatives**”. Ph.D. Thesis, An-Najah N. University, Nablus, (2009).
- [30] <http://en.wikipedia.org/wiki/Anthocyanin> (accessed 26/10/2010).
- [31] D. Ghosh and T. Konishi. “**Anthocyanins and anthocyanin-rich extracts: role in diabetes and eye function**”. *Asia Pac J Clin Nutr*, **16(2)**,(2007), **200**.
- [32]<http://lpi.oregonstate.edu/ss01/anthocyanin.html> (accessed 26/10/2010)
- [33] <http://www.chiro.org/nutrition/FULL/Anthocyanins.shtm>
(accessed 26/10/2010)
- [34] N. J. Cherepy, G. P. Smestad, M.Gra1tzel, and J. Z. Zhang. “**Ultrafast Electron Injection: Implications for a Photoelectrochemical Cell Utilizing an Anthocyanin Dye-Sensitized TiO₂ Nanocrystalline Electrode**”. *Journal of Physical Chemistry B*, **101**, (1997) **9342**.
- [35] P. Vijaybhaskar and A. Ramachandraiah. “**Spectral and Electrochemical Studies of Phenazopyridine**”. *E-Journal of Chemistry*, **6(4)**, (2009), **1181**.
- [36] http://en.wikipedia.org/wiki/Escherichia_coli (accessed 19/5/2011)

[37] <http://www.webmd.com/a-to-z-guides/e-coli-infection-topic-overview>

(accessed 19/5/2011)

[38] S. F. Elena, T. S. Whittam, C. L. Winkworth, M. A. Riley, and R.E. Lenski. “**Genomic divergence of Escherichia coli strains: evidence for horizontal transfer and variation in mutation rates**”. *International Microbiology*, **8**, (2005), **271**.

[39] http://en.wikipedia.org/wiki/Staphylococcus_aureus

(accessed 19/5/2011)

[40] http://www.medicinenet.com/staph_infection/article.htm

(accessed 19/5/2011)

[41] Staph A. H. Bartlett, and K. G. Hulten. “**Staphylococcus aureus Pathogenesis Secretion Systems, Adhesins, and Invasins**”. *Pediatr Infect Dis*, **29**, (2010), **860**.

[42] Y. Bessekhoud, D. Robert, and J. V. Weber. “**Preparation of TiO₂ nanoparticles by Sol-Gel route**”. *International Journal of Photoenergy*, **5**, (2003), **153**.

[43] <http://www.azom.com/article.aspx?ArticleID=5513>

(accessed 22/3/2011).

[44] M. Addamo, M. Bellardita, A. Di Paola and L. Palmisano. **“Preparation and photoactivity of nanostructured anatase, rutile and brookite TiO₂ thin films”**. *Chem. Commun.*, **1**, (2006), **4943**.

[45] <http://www.engr.sjsu.edu/eallen/MatE144/XRD%20Data/NaCl/NaCl.jpg> (accessed 22/3/2011).

[46] R. Ellingson, Atomic and Nuclear Physics Laboratory, (Physics 4780), The University of Toledo. 2010.

[47] J. Yao and C. Wang. **“Decolorization of methylene blue with TiO₂ Sol via UV Irradiation Photocatalytic degradation”**. *International Journal of Photoenergy*, **2010**, (2010), **1**.

[48] S. Dutta, S. A. Parsons, C. Bhattacharjee, P. Jarvis, S. Datta, S. Bandyopadhyay. **“Kinetic study of adsorption and photo-decolorization of Reactive Red 198 on TiO₂ surface”**. *Chemical Engineering Journal*, **155**, (2010), **674**.

[49] M. Rein. **“Copigmentation reactions and color stability of berry anthocyanins”**. *EKT series*, **1331**, (2005), **34**.

[50] A. R. Khataee. **“Photocatalytic removal of C.I. Basic Red 46 on immobilized TiO₂ nanoparticles: Artificial neural network modeling”**. *Environmental Technology*, **30**, (2009), **1155**.

- [51] T. Kim and M. J. Lee. **“Effect of pH and temperature for photocatalytic degradation of organic compound on carbon-coated TiO₂”**. *Journal of Advanced Engineering and Technology*, **3**, (2010), **193**.
- [52] N. Barka, A. Assabbane, A. Nounah, J. Dussaud, Y. Ait Ichou. **“Photocatalytic degradation of methyl orange with immobilized TiO₂ nanoparticles: Effect of pH and some inorganic anions”**. *Physics and Chemistry News* **41** (2008) **85**.
- [53] H. S. Hilal, G. Y.M. Al-Nour, A. Zyoud, M. H. Helal, I. Saadeddin. **“Pristine and supported ZnO-based catalysts for phenazopyridine degradation with direct solar light”**. *Solid State Sciences*, **12**, (2010), **578**.
- [54] N. Barka, A. Assabbane, A. Nounah, Y. Ait Ichou. **“Photocatalytic degradation of indigo carmine in aqueous solution by TiO₂-coated non-woven fibres”**. *Journal of Hazardous Materials*, **152** (2008), **1054**.

جامعة النجاح الوطنية

كلية الدراسات العليا

تنشيط اشباه الموصلات النانوية كحفازات في التحطم الضوئي للعقاقير

والكائنات الدقيقة في الماء

اعداد

فداء طلال عبد القادر صالح

إشراف

أ.د. حكمت هلال

قدمت هذه الأطروحة استكمالاً لمتطلبات درجة الماجستير في الكيمياء بكلية الدراسات العليا في
جامعة النجاح الوطنية في، نابلس- فلسطين.

2011 م

ب

تنشيط أشباه الموصلات النانوية كحفازات في التحطيم الضوئي للعقاقير والكانينات الدقيقة في الماء

إعداد

فداء طلال صالح

إشراف

أ.د. حكمت هلال

الملخص

احتل التحطيم الضوئي للملوثات العضوية في الماء أهمية كبيرة في السنوات الأخيرة وكان أكسيد التيتانيوم TiO_2 من أهم الحفازات الضوئية شبه الموصلة المستخدمة وذلك لأسباب عدة أهمها ثباتيته العالية في الضوء، طبيعته غير السامة، جهده العالي في الأكسدة، وعدم ذائبته في الماء تحت مختلف الظروف. في هذه الدراسة تم تحضير حبيبات أكسيد التيتانيوم النانوية من ثالث كلوريد التيتانيوم $TiCl_3$ ثم تم تحسيسه للضوء المرئي باستخدام صبغة الانثوسيانين الطبيعية المستخلصة من نبات الكركديه. وبعد ذلك تم تثبيت الدقائق الناتجة $TiO_2/anthocyanin$ على أسطح الكربون المنشط (AC). بعد ذلك تم استخدام الناتج $AC/TiO_2/anthocyanin$ كحفاز في تحطيم الفينازوبيريدين كنموذج للملوثات الكيميائية للماء. أما الدقائق $TiO_2/anthocyanin$ فقد استخدمت في دراسة استكشافية أولية من أجل تحطيم البكتيريا مثل E-Coli.

تم تشخيص أكسيد التيتانيوم المحضر باستخدام عدة قياسات لها الأشعة السينية، والميكروسكوب الإلكتروني الماسح ومطيافية الامتصاص الضوئي ومطيافية الانبعاث الوميضي. تم كذلك دراسة تأثير عدة متغيرات على فعالية الحفاز مثل درجة الحرارة ودرجة الحموضة وتركيز الحفاز وتركيز الملوث، حيث وجد أن فعالية الحفاز تزداد بارتفاع درجة الحرارة، درجة الحموضة،

تركيز الحفاز، وتركيز الملوث. كما وجد أن هناك تأثيراً حفزياً لكل من $TiO_2/anthocyanin$ و $AC/TiO_2/anthocyanin$ على التحطيم الضوئي للبكتيريا، إلا أن دراستنا الأولية ركزت على النوع الأول من هذين الحفازين.